

# PROCEEDINGS OF SPIE

[SPIDigitalLibrary.org/conference-proceedings-of-spie](https://spiedigitallibrary.org/conference-proceedings-of-spie)

## Structured polarized light microscopy (SPLM) for mapping collagen fiber orientation of ocular tissues

Bin Yang, Bryn Brazile, Ning-Jiun Jan, Andrew P. Voorhees, Ian A. Sigal

Bin Yang, Bryn Brazile, Ning-Jiun Jan, Andrew P. Voorhees, Ian A. Sigal, "Structured polarized light microscopy (SPLM) for mapping collagen fiber orientation of ocular tissues", Proc. SPIE 10546, Emerging Digital Micromirror Device Based Systems and Applications X, 105460I (22 February 2018); doi: 10.1117/12.2290133

**SPIE.**

Event: SPIE OPTO, 2018, San Francisco, California, United States

# Structured polarized light microscopy (SPLM) for mapping collagen fiber orientation of ocular tissues

Bin Yang<sup>a</sup>, Bryn Brazile<sup>b</sup>, Ning-Jiun Jan<sup>a,b</sup>, Andrew P. Voorhees<sup>a</sup> and Ian A. Sigal<sup>a,b</sup>

<sup>a</sup> Department of Ophthalmology, University of Pittsburgh, Pittsburgh, PA, USA;

<sup>b</sup> Department of Bioengineering, University of Pittsburgh, Pittsburgh, PA, USA

\* [ian@OcularBiomechanics.com](mailto:ian@OcularBiomechanics.com), Phone: 1 412-864-2220

## ABSTRACT

Glaucoma is a disease characterized by progressive and irreversible vision loss leading to blindness. This vision loss is believed to be largely determined by the biomechanics of the optic nerve head region. Optic nerve head biomechanics, in turn, is determined by the properties of the constituent collagen. However, it is challenging to visualize and quantify collagen morphology and orientation *in situ*, and therefore often studies of the region collagen have used histological sections. Here we describe SPLM, a novel imaging technique that combines structured light illumination and polarized light microscopy (PLM) to enable collagen fiber visualization and fiber orientation mapping without requiring tissue sectioning.

We developed a custom automated SPLM imaging system based on an upright microscope and a digital micromirror device (DMD) projector. The high spatial frequency patterns were used to achieve effective background suppression. Enhanced scattering sensitivity with SPLM resulted in images with highly improved visibility of collagen structures, even of tissues covered by pigment. SPLM produced improved fiber orientation maps from superficial layers compared to depth-averaged orientation from regular PLM. SPLM imaging provides valuable information of collagen fiber morphology and orientation *in situ* thus strengthening the study of ocular collagen fiber biomechanics and glaucoma.

**Keywords:** collagen fiber orientation, structured light illumination, polarized light microscopy, ocular tissues, and biomechanics

## 1. INTRODUCTION

Collagen fiber orientation is one of the fundamental properties of ocular tissues, and it plays an important role in the biomechanics of both normal and diseased eyes. It is believed collagen fiber orientation, as well as its biomechanics, are closely associated with several eye diseases[1-3], including glaucoma: a disease characterized by chronic and irreversible vision loss. Recently, polarized light microscopy (PLM) has been applied to study collagen fibers within thin tissue sections [4], providing quantifications with high resolution, large field-of-view and high spatial and angular sensitivities. However, on thick tissues, conventional PLM has limited usefulness because the collagenous eyes tissues are highly scattering. The polarization state of the incident light gets scrambled quickly as it propagates into the tissues. The remitted light retaining useful polarization information is masked by its non-specifically polarized background. Thus, quantifying fiber orientation with conventional PLM is difficult. To overcome such limitation, while preserving advantages of PLM, here we propose, SPLM, a new imaging technique that combines structured light illumination (SLI) with PLM to reduce the non-specific scattering background signals[5], thus allowing collagen fiber orientation mapping on thick ocular tissues.

## 2. METHODS

We developed a custom SPLM imaging platform based on an Olympus upright microscope (Olympus MVX 10). The patterns projected from a digital micromirror device (DMD) (Texas Instruments, LightCrafter) were coupled

into the light-path of the microscope with a 50mm relay lens. Thus, epi-illumination was achieved, and the size of the pattern was de-magnified by the microscope objective. Two polarizers were placed in the illumination and collection paths, respectively, to achieve PLM. To perform SPLM measurements, at each polarization state, three phase-shifted ( $0^\circ$ ,  $120^\circ$  and  $240^\circ$ ) sinusoidal patterns were projected onto the sample and 3 corresponding reflectance images,  $I_1$ ,  $I_2$  and  $I_3$  were acquired by a CMOS camera (Hamamatsu, Flash 4.0 LT). This process was repeated for all 4 polarization states. The pattern projection and image acquisition were automated with a custom program developed in LabVIEW.

From the 3 SLI images, we obtained two derived images, DC and AC, through a demodulation process described in Eq. 1 and 2:

$$I_{dc} = \frac{1}{3}(I_1 + I_2 + I_3) \quad (1)$$

$$I_{ac} = \frac{\sqrt{2}}{3} \left[ \sqrt{(I_1 - I_2)^2 + (I_2 - I_3)^2 + (I_3 - I_1)^2} \right] \quad (2)$$

The DC image is equivalent to the reflectance image under the planar illumination, while the AC image can be considered as background-suppressed image, which has been used in wide-field imaging applications, such as fluorescence imaging[6] and reflected light imaging[5, 7]. With 4 derived images of 4 polarization states, the fiber orientation maps can be obtained using the method we previously described[4]. Both DC and AC versions of fiber orientation maps were computed.

Fresh pig eyes were obtained from a local slaughterhouse and fixed within 6 hours after death by immersion in 10% formalin for 12 hours. After fixation, the eye was cut open coronally, and the posterior pole was retained. Prior to the imaging, the vitreous, retina and pre-lamina neural tissues were carefully removed. Using SPLM, we imaged and quantified collagen fiber orientation of both optic nerve head and sclera observed from the anterior direction. We compared the fiber orientation quantification between SPLM and PLM.

### 3. RESULTS

Figure 1c shows a diagram of a pig eye. The optic nerve head region is located in the posterior pole of the eye and indicated with gray oval. Figure 1a and 1b show both DC and AC images of a fixed pig optic nerve head. The DC image shows collagen beams with low contrast. In some regions, it is difficult to distinguish collagen beams from the surrounding neural tissues. Furthermore, pigments block the visibility of collagen beams that are located under them, as indicated with red arrows in Fig. 1a. In the AC image, the visibility of the collagen beams is greatly improved with neural tissues appearing darker than collagen beams. This is a consequence of the different scattering properties of collagen and neural tissues. Interestingly, the visibility of collagen beams covered by pigments is also greatly enhanced as indicated with red arrows in Fig. 1b. Intensity profiles along the same line for both DC and AC images are shown in Fig. 1d, to demonstrate the background suppression and improved signal-to-background ratio. Although the overall intensity is lower for AC signals, the background is much smaller for AC signal than DC one.

The collagen fiber orientations quantified based on both DC and AC images are shown in Fig. 2a and Fig. 2b, respectively. Collagen fiber orientation is color-coded. Without background suppression (DC), the quantified fiber orientations, shown in Fig. 2a, shows a green hue over all the region. This suggests collagen fibers oriented in the 45-degree direction, which is not true based on prior knowledge[8]. With SLI, Fig. 2b shows a much more heterogeneous fiber orientation map, consistent with previous studies using thin sections. The circumferential fibers along the canal exhibit a rainbow color change over 180-degrees. Also, multiple radial fibers can be identified with color-coded fiber orientation. Even the small-scale undulations of the collagen fibers, or crimp, are clearly visible.

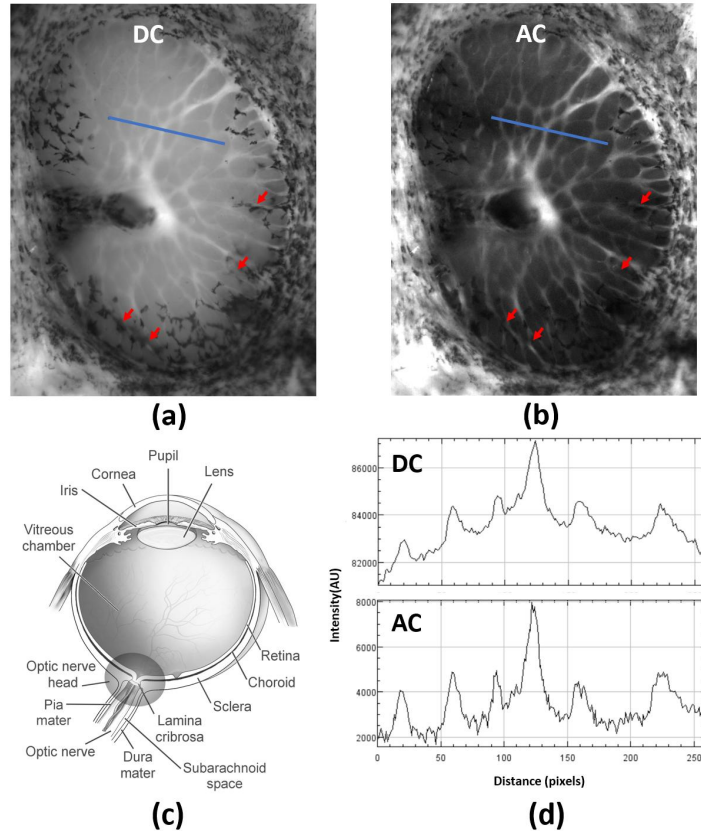


Figure 1 DC (a) and AC (b) images of an uncut pig optic nerve head. Red arrows indicate improved collagen beam's visibility in AC image compared to DC image. (c) Diagram of an eye with gray oval indicating optic nerve head region (adapted from [9]). (d) The intensity profile of a line ROI shows that the AC image has a much lower background signal than the DC image.

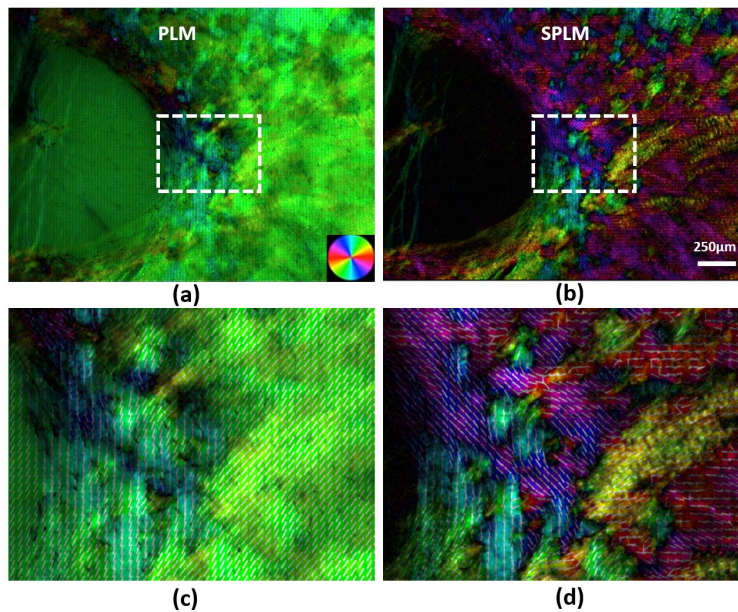


Figure 2 Collagen fiber orientation maps of an uncut thick pig eye tissue in optic nerve head and peripapillary sclera regions based on both PLM and SPLM. (a) shows an overall uniform green color indicating approximately 45-degree fiber orientation,

and it does not agree with prior knowledge; (b) shows a much heterogeneous fiber orientation and both circumferential and radial fibers can be identified based on color-coded orientations; (c) and (d) show detailed orientation vector maps based on PLM and SPLM, respectively, of a small ROI indicated with a dash box.

#### 4. DISCUSSION AND CONCLUSION

In this manuscript, we described SPLM, a new PLM imaging technique that integrates SLI to extend the applicability of PLM from thin sections to uncut thick tissue samples. Under SLI, the scattering tissue acts like a low-pass filter, and high spatial frequency patterns penetrate shallower than lower spatial frequency patterns[10], which effectively eliminates the scattering background from deeper tissue. Thus, the image highlights photons maintaining useful polarization states and are free from scattering background interference, from which, the collagen fiber orientations are quantified

Compared to regular PLM, SPLM can perform collagen fiber quantifications on native thick tissues. By integrating SPLM with mechanical testing devices, it allows us to study not only ocular tissues' microstructures but also their biomechanical functions. Compared to other thick tissue imaging techniques applied to the optic nerve head, such as SALS[11], WAXS[2, 12], SHG[13-15] and OCT[16, 17], SPLM has several advantages, including minimal tissue processing, high spatial and angular resolution and short imaging times. The application of SPLM is not limited to ocular tissues but can be easily extended to other collagenous tissues.

#### ACKNOWLEDGEMENTS

This research work was supported by grants from National Institutes of Health under grants NIH R01-EY023966 and NIH P30-EY008098, Eye and Ear Foundation (Pittsburgh, PA) and Research to prevent blindness (support to the UPMC Department of Ophthalmology).

#### REFERENCES

- [1] J. A. S. Rada, S. Shelton, and T. T. Norton, "The sclera and myopia," *Experimental eye research*, 82(2), 185-200 (2006).
- [2] J. K. Pijanka, B. Coudrillier, K. Ziegler *et al.*, "Quantitative mapping of collagen fiber orientation in non-glaucoma and glaucoma posterior human sclerae/fiber orientation in posterior human sclera," *Investigative ophthalmology & visual science*, 53(9), 5258-5270 (2012).
- [3] G. Wollensak, E. Spoerl, and T. Seiler, "Riboflavin/ultraviolet-A-induced collagen crosslinking for the treatment of keratoconus," *American journal of ophthalmology*, 135(5), 620-627 (2003).
- [4] N.-J. Jan, J. L. Grimm, H. Tran *et al.*, "Polarization microscopy for characterizing fiber orientation of ocular tissues," *Biomedical optics express*, 6(12), 4705-4718 (2015).
- [5] B. Yang, J. Lesicko, M. Sharma *et al.*, "Polarized light spatial frequency domain imaging for non-destructive quantification of soft tissue fibrous structures," *Biomedical optics express*, 6(4), 1520-1533 (2015).
- [6] B. Yang, and J. W. Tunnell, "Real-time absorption reduced surface fluorescence imaging," *Journal of biomedical optics*, 19(9), 090505-090505 (2014).
- [7] B. Yang, J. Lesicko, A. Moy *et al.*, "Color structured light imaging of skin," *Journal of biomedical optics*, 21(5), 050503-050503 (2016).
- [8] N.-J. Jan, C. Gomez, S. Moed *et al.*, "Microstructural Crimp of the Lamina Cribrosa and Peripapillary Sclera Collagen Fibers," *Investigative ophthalmology & visual science*, 58(9), 3378-3388 (2017).

- [9] I. Sigal, J. Grimm, J. Schuman *et al.*, "A method to estimate biomechanics and mechanical properties of optic nerve head tissues from parameters measurable using optical coherence tomography," *IEEE transactions on medical imaging*, 33(6), 1381-1389 (2014).
- [10] D. J. Cuccia, F. Bevilacqua, A. J. Durkin *et al.*, "Quantitation and mapping of tissue optical properties using modulated imaging," *Journal of biomedical optics*, 14(2), 024012-024012-13 (2009).
- [11] M. J. Girard, A. Dahlmann-Noor, S. Rayapureddi *et al.*, "Quantitative mapping of scleral fiber orientation in normal rat eyes," *Investigative ophthalmology & visual science*, 52(13), 9684-9693 (2011).
- [12] C. Boote, J. R. Palko, T. Sorensen *et al.*, "Changes in posterior scleral collagen microstructure in canine eyes with an ADAMTS10 mutation," *Molecular vision*, 22, 503 (2016).
- [13] I. A. Sigal, J. L. Grimm, N.-J. Jan *et al.*, "Eye-Specific IOP-Induced Displacements and Deformations of Human Lamina Cribrosa," *Investigative ophthalmology & visual science*, 55(1), 1-15 (2014).
- [14] S. Ram, F. Danford, S. Howerton *et al.*, "Three-Dimensional Segmentation of the Ex-Vivo Anterior Lamina Cribrosa from Second-Harmonic Imaging Microscopy," *IEEE Transactions on Biomedical Engineering*, (2017).
- [15] E. Cone-Kimball, C. Nguyen, E. N. Oglesby *et al.*, "Scleral structural alterations associated with chronic experimental intraocular pressure elevation in mice," *Molecular vision*, 19, 2023 (2013).
- [16] I. A. Sigal, B. Wang, N. G. Strouthidis *et al.*, "Recent advances in OCT imaging of the lamina cribrosa," *British Journal of Ophthalmology*, 98(Suppl 2), ii34-ii39 (2014).
- [17] B. Wang, H. Tran, M. A. Smith *et al.*, "In-vivo effects of intraocular and intracranial pressures on the lamina cribrosa microstructure," *PloS one*, 12(11), e0188302 (2017).